Which One among Zn(II), Co(II), Mn(II), and Fe(II) is the Most Efficient Ion for the Methionine Aminopeptidase Catalyzed Reaction?

3 AUTHORS, INCLUDING:

Nino Russo
Università della Calabria
512 PUBLICATIONS **7,933** CITATIONS

SEE PROFILE

Marirosa Toscano
Università della Calabria
199 PUBLICATIONS **3,698** CITATIONS

SEE PROFILE

Which One among Zn(II), Co(II), Mn(II), and Fe(II) is the Most Efficient Ion for the Methionine Aminopeptidase Catalyzed Reaction?

Monica Leopoldini, Nino Russo,* and Marirosa Toscano

Contribution from the Dipartimento di Chimica and Centro di Calcolo ad Alte Prestazioni per Elaborazioni Parallele e Distribuite-Centro d'Eccellenza MIUR, Universita' della Calabria, I-87030 Arcavacata di Rende (CS), Italy

Received November 21, 2006; E-mail: nrusso@unical.it

Abstract: The catalytic hydrolysis of a methionyl-peptide substrate by a methionine aminopeptidase active site model cluster was investigated at the DF/B3LYP level of theory, in the gas-phase and in the protein environment. Zn(II), Co(II), Mn(II), and Fe(II) transition metals were examined as the potential catalytic metals of this enzyme involved in protein maturation. Two different mechanisms in which Glu204 was present as protonated or deprotonated residue were considered. The energetic profiles show lower barriers as the protonated glutamate is involved. The rate-determining step of the hydrolysis reaction is always the nucleophilic addition of the hydroxide on substrate carbon, followed by less energetically demanding methionine-peptide C−N bond scission. The lowest activation energy is obtained in the case of zinc dication while the other metals show very high energetic barriers, so that methionine aminopeptidase can be in principle recognized as a dizinc enzyme.

Introduction

Methionine aminopeptidases (MetAPs, EC: 3.4.11.18) are ubiquitous metalloenzymes responsible for the hydrolytic removal of the N-terminal methionine from a newly synthesized polypeptide chain.[1,2] MetAPs belong to a new class of proteases also including aminopeptidase P, creatine amidinohydrolase (creatinase), and prolidase.[2,3] They are specific for N-terminal methionine and act when the formyl group in formylmethionine-peptide is removed by peptide deformylase.[4] MetAPs are involved in cell growth and tumor progression, and their importance increased when type 2 methionine aminopeptidase (MetAP2) was recognized as the molecular target of the TNP-470 and fumagillin antiangiogenesis and antitumor agents.[5,6]

Several structures of MetAPs were solved. *Escherichia coli* MetAP reveals a dimetal center.[3] Two cobalt ions are bound by monodentate His171 and Glu204 and bidentate Asp97, Asp108, and Glu235 residues. A water molecule/hydroxide ion bridges the two cations, and it is thought to act as the nucleophile agent during catalysis.[3]

The physiological metal ions for MetAPs have not been established and remain still controversial. The loss of enzymatic activity upon treatment with EDTA suggested MetAP to be a metalloenzyme.[7] Activity was observed in the presence of different metals such as Co(II) and Zn(II) in the case of *Escherichia coli* MetAP-Ia;[7,8] Co(II), Zn(II), Mn(II), and Ni-(II) for yeast MetAP-Ib;[9] Co(II) for yeast MetAP-IIa;[10] and Co-(II) and Mn(II) for human MetAP-IIb.[11] Several experiments were devoted to the elucidation of the physiological metal. Yeast MetAP-Ib, reconstituted with a low concentration of Zn(II), was shown to be as active as the Co(II)-substituted enzyme, while higher concentrations of zinc were inhibitory.[9] The high activity of the yeast enzyme in the presence of Zn(II), in contrast to the lack of activity in the presence of Co(II) and a physiological concentration of reduced glutathione, suggested that Zn(II) may be the most relevant catalytic cation.[9] However, on the basis of experiments performed anaerobically, D'souza and Holz[12] suggested that Fe(II) may be the physiological metal for *E. coli* MetAP. They found that Co(II) and Fe(II) give the highest activity. In addition, their analysis of the metal content of bacterial extracts without and with the plasmid-based overexpression of MetAP showed that the level of Fe(II) increases significantly in the latter case. In contrast, an analysis of the metal content of endogenous and recombinant *Pyrococcus furiosis* prolidase suggested Co(II) to be the biologically relevant metal.[13]

(1) Bradshaw, R. A.; Brickey, W. W.; Walker, K. W. *Trends Biochem. Sci.* **1998**, *23*, 23−267.
(2) Lowther, W. T.; Matthews, B. W. *Biochim. Biophys. Acta* **2000**, *1477*, 157−167.
(3) Roderick, S. L.; Matthews, B. W. *Biochemistry* **1993**, *32*, 3907.
(4) Solbiati, J.; Chapman-Smith, A.; Miller, J. L.; Miller, C. G.; Cronan, J. E., Jr. *J. Mol. Biol.* **1999**, *290*, 607−614.
(5) Griffith, E. C.; Su, Z.; Turk, B. E.; Chen, S.; Chang, Y. H.; Wu, Z.; Biemann, K.; Liu, J. O. *Chem. Biol.* **1997**, *4*, 461−471.
(6) Sin, N.; Meng, L.; Wang, M. Q.; Wen, J. J.; Bornmann, W. G.; Crews, C. M. *Proc. Natl. Acad. Sci. U.S.A.* **1997**, *1094*, 6099−6103.

(7) Ben-Bassat, A.; Bauer, K.; Chang, S. Y.; Myambo, K.; Boosman, A.; Chang, S. *J. Bacteriol.* **1987**, *169*, 751−757.
(8) Lowther, W. T.; Orville, A. M.; Madden, D. T.; Lim, S.; Rich, D. H.; Matthews, B. W. *Biochemistry* **1999**, *38*, 7678−7688.
(9) Walker, K. W.; Bradshaw, R. A. *Protein Sci.* **1998**, *7*, 2684−2687.
(10) Chang, Y. H.; Teichert, U.; Smith, J. A. *J. Biol. Chem.* **1992**, *267*, 8007−8011.
(11) Li, X.; Chang, Y. H. *Biochem. Biophys. Res. Commun.* **1996**, *227*, 152−159.
(12) D'souza, V. M.; Holz, R. C. *Biochemistry* **1999**, *38*, 11079−11085.

Scheme 1. Catalytic Mechanism of Methionine Aminopeptidase
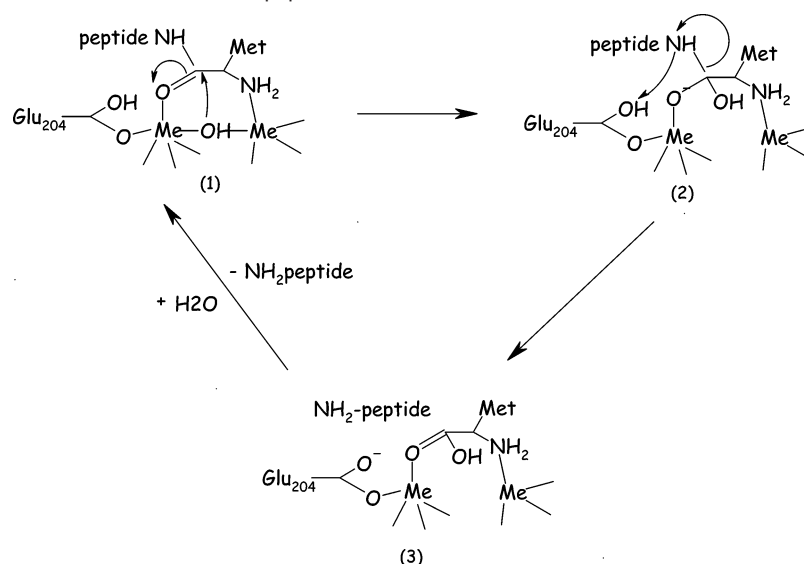
At this time, it is still unclear which one may represent the catalytic ion.

On the basis of inhibition and mutation studies, and of data concerning related enzymes, a reaction mechanism was proposed.[8,14] Substrate binds to one metallic center by the NH_2 terminal group, while the other cation interacts with the substrate carbonyl oxygen atom. Nucleophilic addition of the bridging hydroxide on the methionine-peptide carbonyl carbon leads to a tetrahedral intermediate, whose protonation on nitrogen finally entails the scission of the substrate C—N bond (see Scheme 1).

Glu204 is a general acid/base catalyst. It acts as a base by abstracting an H^+ from the bridging water molecule generating the $^-$OH nucleophile and as an acid by protonating the nitrogen atom in the substrate. Its role as proton shuttle is similar to that proposed for Glu133 in peptide deformylase,[15] Glu270 in carboxypeptidase A,[16,17] Asp120 in β-lactamase,[18] and Glu106 in carbonic anhydrase.[19]

The protonation state of the glutamate residue is not well established. In the X-ray 2.4 Å resolved structure of the *E. coli* MetAP free enzyme,[3] the O_{Glu204}—Co^{2+} distance of 1.6 Å may be seen as an indication of an ionized residue. However, this crystal structure does not show water molecule nucleophiles between the two cations. Instead, in another 1.9 Å Co-containing free enzyme structure[8] involving an oxygen atom between the two Co^{2+}, the O_{Glu204}—Co^{2+} distance of 2.09 Å could be more indicative for a neutral glutamate.

Some additional aminoacids were identified as important residues in achieving catalysis.[20–23] In particular, the residues

His178 and His79, even if not directly involved, help in stabilizing substrate binding and the transition state, by establishing a H-bond with the carbonyl oxygen (His178) and with the nitrogen (His79) of the substrate.

The reaction sequence proposed for MetAP is typical of metallohydrolases such as mononuclear peptide deformylase,[15] thermolysin[24] and carboxypeptidase,[16,17] and dinuclear leucine aminopeptidase, arginase, and *Aeromonas proteolytica* aminopeptidase.[25]

With the purpose of identifying the catalytic metal dication among zinc, cobalt, manganese, and iron, we have performed a computational study on the hydrolysis of a peptide-methionine substrate by a dinuclear cluster as a model for the MetAP active site. As mentioned before, two different models for the Glu204 residue, that is neutral and ionized, were examined in order to establish the energetically favored mechanism.

Computational Details

All the computations reported in this study were carried out with the Gaussian 03 code,[26] employing the hybrid Becke exchange and Lee, Yang, and Parr correlation (B3LYP) functionals.[27–30] The performance of the DF-B3LYP method in predicting properties of transition metals containing systems is satisfactory and supported by a considerable amount of literature papers, also concerning enzymatic catalysis, including closed-[19,31,32,40] and open -shell structures.[15,33–39,41] For

(13) Ghosh, M.; Grunden, A. M.; Dunn, D. M.; Weiss, R.; Adams, M. W. W. *J. Bacteriol.* **1998**, *180*, 4781–4789.
(14) Lowther, W. T.; Zhang, Y.; Sampson, P. B.; Honek, J. F.; Matthews, B. W. *Biochemistry* **1999**, *38*, 14810–14819.
(15) Leopoldini, M.; Russo, N.; Toscano, M. *J. Phys. Chem. B* **2006**, *110*, 1063–1072.
(16) Abashkin, Y. G.; Burt, S. K.; Collins, J. R.; Cachau, R. E.; Russo, N.; Erickson, J. W. In *Metal-Ligand Interactions: Structure and Reactivity*; Russo, N., Salahub, D. R., Eds.; Nato Science Series; Kluwer: Dordrecht, 1996; Vol. 474, pp 1–22.
(17) Bertini, I.; Luchinat, C. In *Bioinorganic Chemistry*; Bertini, I., Gray, H. B., Lippard, S. J., Valentine, J. S., Eds.; University Science Books: Mill Valley, CA, 1994.
(18) Olsen, L.; Anthony, J.; Ryde, U.; Adolph, H. W.; Hemmingsen, L. *J. Phys. Chem. B* **2003**, *107*, 2366–2375.
(19) Marino, T.; Russo, N.; Toscano, M. *J. Am. Chem. Soc.* **2005**, *127*, 4242–4253.

(20) Wilce, M. C.; Bond, C. S.; Dixon, N. E.; Freeman, H. C.; Guss, J. M.; Lilley, P. E.; Wilce, J. A. *Proc. Natl. Acad. Sci. U.S.A.* **1998**, *95*, 3472–7347.
(21) Coll, M.; Knof, S. H.; Ohga, Y.; Messerschmidt, A.; Huber, R.; Moellering, H.; Russmann, L.; Schumacher, G. *J. Mol. Biol.* **1990**, *214*, 597–610.
(22) Silverman, D. N.; Lindskog, S. *Acc. Chem. Res.* **1988**, *21*, 30–36.
(23) Christianson, D. W.; Fierke, C. A. *Acc. Chem. Res.* **1996**, *29*, 331–333.
(24) Pelmenschikov, V.; Blomberg, M. R. A.; Siegbahn, P. E. M. *J. Biol. Inorg. Chem.* **2002**, *7*, 284–298.
(25) Lipscomb, W. N.; Strater, N. *Chem. Rev.* **1996**, *96*, 2375–2433.
(26) Frisch, M. J., et al. *Gaussian 03*; Gaussian, Inc.: Pittsburgh PA, 2003.
(27) Becke, A. D. *J. Chem. Phys.* **1993**, *98*, 5648–5652.
(28) Lee, C.; Yang, W.; Parr, R. G. *Phys. Rev. B* **1988**, *37*, 785–789.
(29) Becke, A. D. *J. Chem. Phys.* **1993**, *98*, 1372.
(30) Becke, A. D. *Phys. Rev. B* **1988**, *38*, 3098.
(31) Hall, M. B.; Webster, C. E. *J. Am. Chem. Soc.* **2001**, *123*, 5820–5821.
(32) Friesner, R. A.; Beachy, M. D. *Curr. Opin. Struct. Biol.* **1998**, *8*, 257–262.
(33) Siegbahn, P. E. M.; Blomberg, M. R. A. *Annu. Rev. Phys. Chem.* **1999**, *50*, 221–249.
(34) Bernardi, F.; Bottoni, A.; Casadio, R.; Fariselli, P.; Rigo, A. *Int. J. Quantum Chem.* **1996**, *58*, 109–119.

instance, the applicability of different density functional methods for molecules containing transition metals was widely checked, by computing the binding energies of CO ligands in several metal carbonyl complexes for which reasonably accurate experimental results were available. Results[42−46] showed that, for the B3LYP functional, the errors are of the same size as the experimental error bars (about 2.0 kcal/mol)

For the geometry optimization, the 6-311+G** basis set[47−50] was used for the C, N, O, S, and H atom representation, while for the metallic dications the LANL2DZ pseudopotential[51] was employed. Frequency calculations were performed at the same level of theory on all the stationary points of the reaction path to establish their character of minima or saddle points. Zero-point energy corrections, obtained from the vibrational analysis, were then included in all the relative energy values.
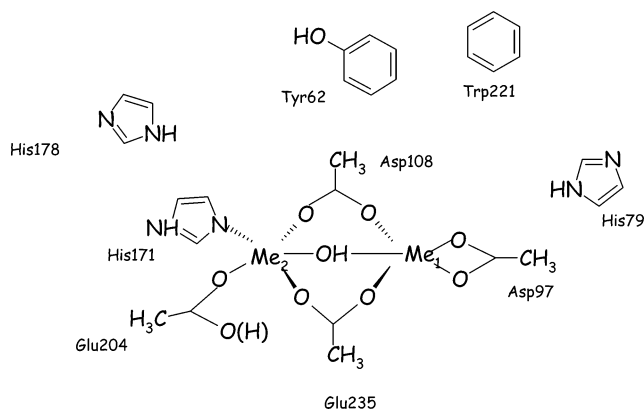
Intrinsic reaction coordinate (IRC) calculations[52,53] were performed with the aim to confirm that a given transition state connects a particular couple of consecutive minima.

The check of stability for all open-shell optimized structure wave functions was carried out by means of the Stable procedure[54−56] implemented in G03 code.

No spin contamination was found for the open-shell systems, being that the $\langle S^2 \rangle$ values after annihilation for all the stationary points are those expected for the considered multiplicities (12.0 for Co^{2+} septets, 20.00 for Fe^{2+} nonets, and 30.00 for Mn^{2+} undecaplets).

Solvent effects were computed in the framework of the Self-Consistent Reaction Field Polarizable Continuum Model[57−59] in which the cavity is created *via* a series of overlapping spheres, using the CPCM[60,61] polarizable conductor calculation model. The UFF radii from the UFF force field[62] were used to build the cavity, in the gas-phase equilibrium geometry. The dielectric constant value $\epsilon = 4$ was chosen by taking into account the coupled effect of the protein itself and the

(35) Bernardi, F.; Bottoni, A.; Casadio, R.; Fariselli, P.; Rigo, A. *Inorg. Chem.* **1996**, *35*, 5207−5212.
(36) Flock, M.; Pieloot, K. *J. Phys. Chem. A* **1999**, *103*, 95−102.
(37) Lind, T.; Siegbahn, P. E. M.; Crabtree, R. H. *J. Phys. Chem.* **1999**, *103*, 1193−1202.
(38) Siegbahn, P. E. M.; Blomberg, M. R. A. *Chem. Rev.* **2000**, *100*, 421−437.
(39) Noodleman, L.; Lovell, T.; Han, W. G.; Li, J.; Himo, F. *Chem. Rev.* **2004**, *104*, 459−508.
(40) Leopoldini, M.; Russo, N.; Toscano, M. *Chem.—Eur. J.* **2006**, DOI 10.1002/chem.200601123.
(41) Leopoldini, M.; Russo, N.; Toscano, M.; Dulak, M.; Wesoloski, A. T. *Chem.—Eur. J.* **2006**, *12*, 2532−2541.
(42) Ricca, A.; Bauschlicher, C. W., Jr. *J. Phys. Chem.* **1994**, *98*, 12899−12903.
(43) Sunderlin, L. S.; Wang, D.; Squires, R. R. *J. Am. Chem. Soc.* **1992**, *114*, 2788.
(44) Blomberg, M. R. A.; Siegbahn, P. E. M.; Svensson, M. *J. Chem. Phys.* **1996**, *104*, 9546−9554.
(45) Koch, W.; Hertwig, R. H. In *Encyclopedia of Computational Chemistry*; Schleyer, P. v. R., Ed.; Wiley: Chichester, 1998.
(46) Li, J.; Schreckenbach, G.; Ziegler, T. *J. Phys. Chem.* **1994**, *98*, 4838−4841.
(47) Ditchfield, R.; Hehre, W. J.; Pople, J. A. *J. Chem. Phys.* **1971**, *54*, 724−728.
(48) Hehre, W. J.; Ditchfield, R.; Pople, J. A. *J. Chem. Phys.* **1972**, *56*, 2257−2261.
(49) Hariharan, P. C.; Pople, J. A. *Mol. Phys.* **1974**, *27*, 209−214.
(50) Gordon, M. S. *Chem. Phys. Lett.* **1980**, *76*, 163−168.
(51) (a) Hay, P. J.; Wadt, W. R. *J. Chem. Phys.* **1985**, *82*, 270−283. (b) Hay, P. J.; Wadt, W. R. *J. Chem. Phys.* **1985**, *82*, 284−298. (c) Hay, P. J.; Wadt, W. R. *J. Chem. Phys.* **1985**, *82*, 299−310.
(52) Gonzalez, C.; Schlegel, H. B. *J. Chem. Phys.* **1989**, *90*, 2154.
(53) Gonzalez, C.; Schlegel, H. B. *J. Phys. Chem.* **1990**, *94*, 5523.
(54) Seeger, R.; Pople, J. A. *J. Chem. Phys.* **1977**, *66*.
(55) Bauernschmitt, R.; Ahlrichs, R. *J. Chem. Phys.* **1996**, *104*, 9047.
(56) Schlegel, H. B.; McDouall, J. J. In *Computational Advances in Organic Chemistry*; Ogretir, C., Csizmadia, I. G., Eds.; Kluwer Academic: The Netherlands, 1991; pp 167−185.
(57) Miertus, S.; Scrocco, E.; Tomasi, J. *Chem. Phys.* **1981**, *55*, 117−129.
(58) Miertus, S.; Tomasi, J. *Chem. Phys.* **1982**, *65*, 239−245.
(59) Cossi, M.; Barone, V.; Commi, R.; Tomasi, J. *Chem. Phys. Lett.* **1996**, *255*, 327.
(60) Barone, V.; Cossi, M. *J. Phys. Chem. A* **1998**, *102*, 1995−2001.
(61) Cossi, M.; Rega, N.; Scalmani, G.; Barone, V. *J. Comput. Chem.* **2003**, *24*, 669−681.
(62) Barone, V.; Cossi, M.; Menucci, B.; Tomasi, J. *J. Chem. Phys.* **1997**, *107*, 3210−3221.

Scheme 2. Model Cluster Used for the Simulation of MetAP Active Site[a]

[a] The (H) stands for protonated/deprotonated Glu204.

water medium surrounding the protein, according to previous suggestions.[15,19,38−41]

The model cluster used to simulate the active site of MetAP (see Scheme 2) was built starting from the 1.8 Å X-ray structure of *E. coli* methionine aminopeptidase in complex with the methionine product (pdb code = 1C21).[14] The first shell coordination sphere of dications was reproduced by three CH_3COO^- negative groups that simulate the Asp97, Asp108, and Glu235 residues and an imidazole ring that mimics the His171 amino acid. A CH_3COOH neutral molecule and a hydroxyl group were used for modeling the Glu204 residue and the bridging −OH nucleophile, respectively. This protonation scheme is supported by several theoretical works[15,16,18,19] concerning metallohydrolases, according to which the metal-bound water molecule is deprotonated to −OH by general glutamate residues, providing the nucleophile agent. However, since the presence of negative Glu204 was questioned by reviewers, both protonation states for Glu204 were taken into account. The mechanism is referred to as A or B depending on whether it involves a neutral or an ionized residue, respectively.

Two imidazoles, a benzene, and a phenol are included as simplified models of the nearby residues His79, His178, Trp221, and Tyr62, respectively. The $CH_3NHC=OCH(NH_2)CH_2CH_2SCH_3$ molecule was used to imitate the peptide-methionine substrate. No water molecule was used for reproducing the Co1 coordination number[8] because this is replaced by substrate NH_2 during catalysis. An H-atom of each amino acidic residue was kept frozen at its crystallographic position in order to mimic the steric effects produced by the surrounding protein and to avoid an unrealistic expansion of the cluster during the optimization procedure. The substrate and products were left free from constraints during the optimization procedure.

Natural Bond Orbital (NBO) analysis[63] was carried out to determine net charges and some electronic properties.
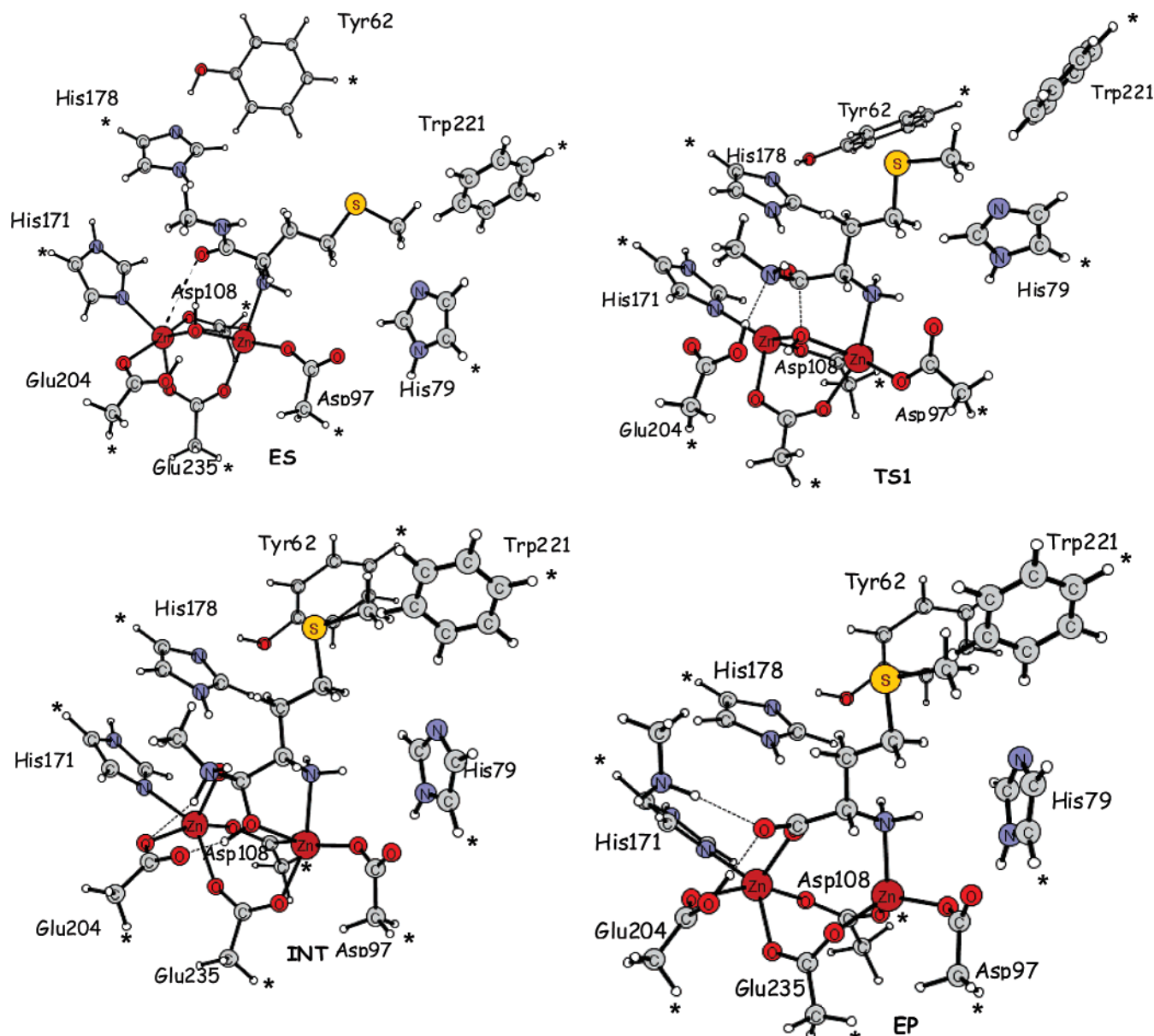
Results and Discussion

Mechanism A. Protonated Glu204. The minimized structures of all the stationary points belonging to the reaction catalytic sequence of Scheme 1 for mechanism A are sketched in Figure 1, for zinc, cobalt, manganese, and iron cations. The main geometrical parameters are collected in Table 1.

The complex between the enzyme active site and the substrate, ES, is obtained when the methionine-peptide interacts with the Me1 metal center through the amide NH_2 lone pair (Me1−N distances are 2.35, 2.24, 2.36, and 2.28 Å, for zinc, cobalt, manganese, and iron, respectively). The carbonyl oxygen of the substrate establishes with Me2 a long-range interaction

(63) Glendening, E. D.; Reed, A. E.; Carpenter, J. E.; Weinhold, F. *NBO*, version 3.1.

Figure 1. Equilibrium geometries of the stationary points ES, TS, INT, and EP belonging to mechanism A.

for all considered metal species (O−Me2 distance is 3.91, 4.36, 4.48, and 4.51 Å, for zinc, cobalt, manganese, and iron, respectively), and it is involved in a H-bond with the bridging OH (1.92, 2.23, 2.25, and 2.18 Å) that in turn engages a hydrogen bond with the protonated Glu204 residue (1.55, 1.55, 1.56, and 1.57 Å). The O−Me2 distance values (Table 1) indicate that a slight polarization in the substrate could be possible only in the case of zinc.

Following the proposal of the reaction mechanism, the nucleophilic attack (TS in Figure 1) by the bridging ⁻OH to the carbonyl C atom in the methionine-peptide is found for the O−C distance value that is 1.86, 1.79, 1.91, and 1.90 Å, for zinc, cobalt, manganese, and iron, respectively (see Table 1).

The hybridization of the substrate C atom changes from sp^2 to sp^3 while amide C−N and carbonyl C=O bonds lengthen up to 1.44 and 1.27 Å (Zn^{2+}), 1.45 and 1.27 Å (Co^{2+}), 1.43 and 1.27 Å (Mn^{2+}), and 1.43 and 1.27 Å (Fe^{2+}). For all dications considered, the formation of the bond between the nucleophile and the substrate C atom entails the approach of the carbonyl

oxygen to the Me2 center, but the substrate terminal NH_2 retains its bond with Me1. In this TS, the Glu204 coordinated to Me2 moves away from the metallic center and reorientates itself in order to strongly interact by a H-bond with the amide NH.

An imaginary frequency at 189, 183, 197 and 208 cm⁻¹, for zinc, cobalt, manganese and iron, respectively, corresponds mainly to the stretching of the incoming bond between the OH and the carbonyl carbon, and to a lesser degree to the shift of the Glu204 proton toward the amide NH.

The hydrogen bond between the carbonyl oxygen and the His178 residue, together with that involving the terminal NH_2 group and Asp97, has a stabilizing effect on the TS.

After the transition state TS, the reaction proceeds through the formation of the stable intermediate INT.

The O_{OH}−C bond is completely formed (1.41, 1.42, 1.41, and 1.42 Å, for Zn^{2+}, Co^{2+}, Mn^{2+}, and Fe^{2+}, in this order), and the amide nitrogen is protonated by the Glu204 residue that in turn re-approaches to the Me2 center (2.12, 2.08, 2.17, and 2.05 Å, for Zn^{2+}, Co^{2+}, Mn^{2+}, and Fe^{2+}, respectively). The

Table 1. Main Geometrical Parameters of Intermediates and Transition State of Mechanism A, for Zinc, Cobalt, Manganese, and Iron

|	ES	TS	INT	EP
$Zn1-NH_{2sub}$	2.35	2.20	2.24	2.14
$Zn2-O_{sub}$	3.91	2.48	2.12	2.05
$Zn2-O_{Glu204}$	2.36	3.35	2.12	2.22
$O_{OH}-C_{sub}$	3.48	1.86	1.41	1.25
$C_{sub}-O_{sub}$	1.24	1.27	1.30	1.28
$C_{sub}-N_{sub}$	1.36	1.44	1.68	3.96
$Co1-NH_{2sub}$	2.24	2.17	2.21	2.11
$Co2-O_{sub}$	4.36	2.43	2.11	2.02
$Co2-O_{Glu204}$	2.25	3.36	2.08	2.27
$O_{OH}-C_{sub}$	3.28	1.79	1.42	1.24
$C_{sub}-O_{sub}$	1.24	1.27	1.30	1.29
$C_{sub}-N_{sub}$	1.35	1.45	1.68	3.93
$Mn1-NH_{2sub}$	2.36	2.31	2.33	2.22
$Mn2-O_{sub}$	4.48	2.38	2.20	2.12
$Mn2-O_{Glu204}$	2.33	3.25	2.17	2.25
$O_{OH}-C_{sub}$	3.31	1.91	1.41	1.25
$C_{sub}-O_{sub}$	1.24	1.27	1.30	1.28
$C_{sub}-N_{sub}$	1.35	1.43	1.69	4.12
$Fe1-NH_{2sub}$	2.28	2.23	2.26	2.18
$Fe2-O_{sub}$	4.51	2.37	2.17	2.03
$Fe2-O_{Glu204}$	2.31	3.23	2.05	2.22
$O_{OH}-C_{sub}$	3.35	1.90	1.42	1.24
$C_{sub}-O_{sub}$	1.24	1.27	1.30	1.29
$C_{sub}-N_{sub}$	1.35	1.43	1.66	4.01

C−N σ bond in the substrate is computed to be 1.68 (zinc), 1.68 (cobalt), 1.69 (manganese), and 1.66 Å (iron). As in the case of TS, the methionine-peptide carbonyl oxygen establishes a H-bond with the His178 amino acid. The negative oxygen atom of the Glu204 residue appears to involve two hydrogen bonds with the original nucleophile OH and the protonated NH_2 (see Figure 1). The oxygen of the OH group remains always coordinated to the Me1, for all considered metal centers.

All attempts to localize a saddle point for the cleavage of the C−N coupled to the protonation of the Glu204 residue failed, so that we have hypothesized that the breaking of this bond, leading to the final EP complex among the enzyme, the methionine, and the CH_3NH_2 leaving group (see Figure 1), must occur in a barrierless step. The product methionine is bound to the active site through both the NH_2 and the CO groups (2.14 and 2.05 Å for Zn^{2+}, 2.11 and 2.02 Å for Co^{2+}, 2.22 and 2.12 Å for Mn^{2+}, and 2.18 and 2.03 Å for Fe^{2+}). The neutral Glu204 amino acid is engaged in a hydrogen bond with the other oxygen atom in methionine. The CH_3NH_2 appears to be bound to the active site because of the weak interaction between its NH_2 and the oxygen of methionine (see Figure 1).

The findings for MetAP are quite similar to those obtained for the hydrolysis achieved by peptide deformylase[15] and thermolysin[24] metalloenzymes. For these, the whole reaction is made up by the nucleophilic addition on the carbon atom in substrate coupled to the protonation of the amide group. The cleavage of the C−N bond that gives rise to the final products occurs as a barrierless step.

The Potential Energy Surfaces (PESs) for the hydrolysis, in the gas phase and in the protein environment, of the $CH_3NHC=OCH(NH_2)CH_2CH_2SCH_3$ substrate by the model cluster with neutral Glu204 (see Scheme 2) are reported in Figure 2.

The energy cost (TS) to pass from the initial ES complex to the tetrahedral intermediate INT is computed to be 16.8 kcal/
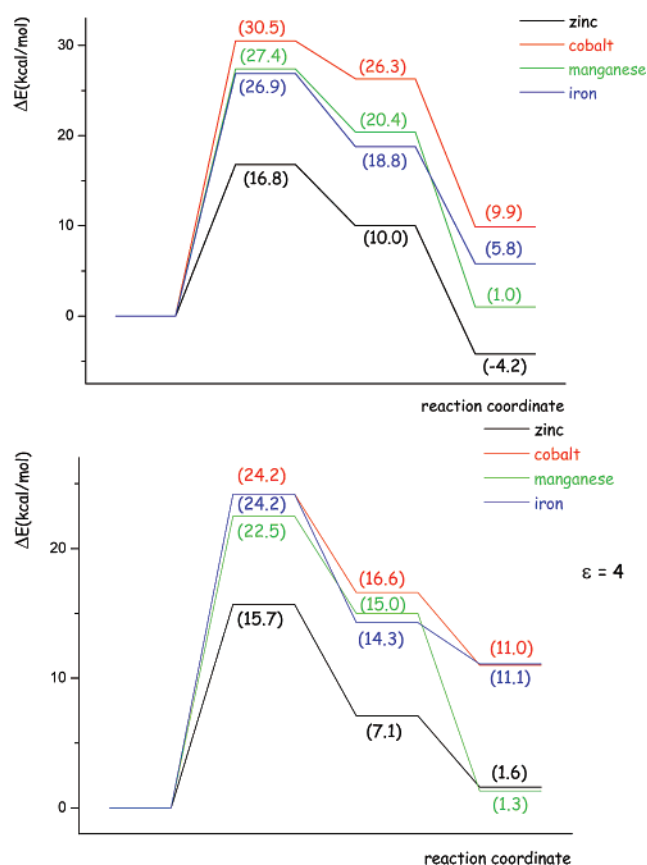
Figure 2. Mechanism A potential energy surfaces for hydrolysis of methionyl-peptide by MetAP, for Zn^{2+} (black line), Co^{2+} (red line), Mn^{2+} (green line), and Fe^{2+} (blue line), in the gas phase (on the top) and in the protein environment (on the bottom).

mol for the Zn^{2+} cation and 30.5, 27.4, and 26.9 kcal/mol for Co^{2+}, Mn^{2+}, and Fe^{2+}, respectively. These values indicate that the nucleophilic attack that determines the reaction kinetics proceeds with a reasonable rate only in the case of the zinc metal, while the other cations show activation barriers that are not compatible with an enzymatic catalysis.

The INT stationary point is located, along the potential energy profile, at 10.0, 26.3, 20.4, and 18.8 kcal/mol, for zinc, cobalt, manganese, and iron cations, in this order.

From this intermediate, the final complex EP among the active site, the methionine, and the CH_3NH_2 originates without an activation barrier. It is found at 1.0, 9.9, and 5.8 kcal/mol above the reactants ES, in the case of Co(II), Mn(II), and Fe(II), while it lies 4.2 kcal/mol below the reference for Zn(II). Thus, the catalyzed reaction in the gas phase results in being exothermic only for the zinc cation, and it is thermodynamically unfavored especially for Co^{2+} and Mn^{2+} (Figure 2).

The computations in the protein environment in which we have used the value of $\epsilon = 4$ point out a more marked energetic stabilization of intermediate with respect to that of the transition state for all the cations considered. The activation energy values, required to overcome the TS, of 15.7 (Zn^{2+}), 24.2 (Co^{2+}), 22.5 (Mn^{2+}), and 24.2 (Fe^{2+}) kcal/mol indicate that the energetic decrease caused by the surrounding protein is more meaningful for cobalt and manganese cations (6.3 and 4.9 kcal/mol in going from the gas to the condensed phase) rather than for zinc and iron (1.1 and 2.7 kcal/mol, respectively).

Table 2. Atomic Net Charges (in |e|) of the Stationary Points along the Potential Energy Surface of Methionine Aminopeptidase

atom	Zn(II)	Co(II)	Mn(II)	Fe(II)
		ES		
Me1	1.68	1.45	1.53	1.45
Me2	1.67	1.45	1.53	1.46
O$_{OH}$	−1.28	−1.18	−1.21	−1.19
C$_{sub}$	0.70	0.71	0.71	0.72
O$_{sub}$	−0.68	−0.73	−0.72	−0.72
N$_{sub}$	−0.65	−0.62	−0.62	−0.62
		TS		
Me1	1.67	1.43	1.52	1.45
Me2	1.66	1.46	1.55	1.48
O$_{OH}$	−1.10	−1.01	−1.07	−1.05
C$_{sub}$	0.76	0.77	0.77	0.77
O$_{sub}$	−0.83	−0.84	−0.83	−0.82
N$_{sub}$	−0.74	−0.75	−0.73	−0.73
		INT		
Me1	1.68	1.46	1.53	1.45
Me2	1.68	1.48	1.55	1.49
O$_{OH}$	−0.87	−0.86	−0.86	−0.84
C$_{sub}$	0.79	0.79	0.79	0.79
O$_{sub}$	−0.94	−0.89	−0.90	−0.90
N$_{sub}$	−0.70	−0.70	−0.70	−0.70
		EP		
Me1	1.68	1.42	1.53	1.44
Me2	1.68	1.47	1.55	1.48
O$_{OH}$	−0.89	−0.85	−0.85	−0.86
C$_{sub}$	0.87	0.87	0.86	0.87
O$_{sub}$	−0.73	−0.72	−0.75	−0.72
N$_{sub}$	−0.92	−0.92	−0.92	−0.92

The intermediate INT is found at 7.1 (Zn^{2+}), 16.6 (Co^{2+}), 15.0 (Mn^{2+}), and 14.3 (Fe^{2+}) kcal/mol above the reactants asymptote.

The protein environment effect seems to slightly destabilize the hydrolysis products. The Zn(II) and Mn(II) containing EP complexes lying at 1.6 and 1.3 kcal/mol above the reactants are practically isoenergetic as well as Fe(II) and Co(II) containing ones that are found at 11.0 and 11.1 kcal/mol above the references.

The PESs for the four cations show clearly that the most favorite candidate to perform the hydrolysis of the methionine-peptide substrate is the dizinc cluster. In fact, the rate-determining step of the nucleophilic attack requires an activation energy of 16.8 and 15.7 kcal/mol in the gas phase and in the protein environment, respectively.

The cobalt cation that was claimed out as the most probable physiological metal for MetAP involves activation energies of 30.5 (*in vacuo*) and 24.2 kcal/mol (in the protein) that are too high as compared to those normally implicated in enzymes catalyzed reactions.

The order of the catalytic activity is Zn > Fe > Mn > Co, in the gas phase. It becomes Zn > Mn > Fe = Co when the protein environment is considered.

With the aim to better understand the different activity of these metal cations in the catalysis, the Natural Bond Orbital (NBO) analysis was performed on all the stationary points along the reaction profiles of the Zn, Co, Mn, and Fe dinuclear cluster. Results concerning natural atomic net charges are collected in Table 2.

The values of this table convey that, in the Zn-ES species, the nucleophile has the highest charge density due to the character being essentially ionic of the bond established with the two metals. The greater the negative charge on the

nucleophile, the easier the addition on the substrate positive carbonyl carbon will be. In the other metal clusters, the covalent character becomes more important than in the case of the zinc ion, as the deviation from the +2 initial charge value indicates. It is worth noting that the Zn-ES complex shows a minor number of H-bonds with respect to the analogous Co-ES intermediate. This means that, in the case of zinc, the ES complex is less stabilized than in the case of cobalt and its energy is closer to that of the next TS, so that the clearing of the barrier is easier for the former.

The results concerning the energetics of the reaction found here for methionine aminopeptidase enzyme are different from those obtained for peptide deformylase,[15] for which also two catalytic metal cations were hypothesized, i.e., Zn and Fe. The B3LYP findings for peptide deformylase indicated[15] that both the metallic forms of the enzyme induce almost the same polarization on the nucleophile and the substrate, so to have activation energies very similar. Instead, MetAP results in being more strongly active when the Zn^{2+} ion is involved.

Mechanism B. Deprotonated Glu204. Within the mechanism B, we have decided to test the catalytic capability of zinc and cobalt because these two cations are recognized as the most probable metals present *in vivo*. The minimized structures of all the stationary points belonging to the reaction catalytic sequence of Scheme 1 are sketched in Figure 3. Main geometrical parameters are collected in the Table 3. The corresponding Potential Energy Surfaces are depicted in Figure 4.

Reaction starts with the formation of the methionine−enzyme complex, ES′. With respect to the previous path, the methionine rearranges itself in such a way that a hydrogen bond is established between the amide nitrogen (donor) and the OH nucleophile (acceptor). In this case, no coordination of the substrate carbonyl oxygen to the Me2 center occurs, in contrast to the experimental suggestions,[3,8,14] while the coordination of the terminal NH_2 group at the Me1 center is retained (N−Me distance is 2.46 and 2.42 Å, for Zn and Co).

In the transition state for the nucleophilic addition on the carbonyl carbon (TS1′), the O_{OH}−C_{sub} distance assumes a value of 1.80 (Zn) and 1.84 Å (Co). The imaginary frequency at 158 and 149 cm^{-1} corresponds to the formation of the C−O_{OH} bond.

For both dication clusters, TS1′ evolves into the INT1′ intermediate. This species is characterized by a C_{sub}−O_{OH} bond of 1.48 (for zinc) and 1.49 Å (for cobalt). The OH points toward the Glu204 O2δ negative oxygen, establishing a H-bond of length 1.65 Å in both cases.

Through TS2′, the proton moves from the nucleophile to the glutamate residue. The animation of the imaginary frequency at 377 (for zinc) and 392 (for cobalt) cm^{-1} indicates mainly the motion of the H−O_{OH} and H−O_{Glu} couple of bonds (critical distances are 1.29 and 1.16 Å, and 1.34 and 1.12 Å, for zinc and cobalt, respectively). Contrary to what is encountered for mechanism A, in mechanism B involving the ionized glutamate, the nucleophile addition and the proton shift from the OH to the Glu204 appear not to be concerted.

In the intermediate INT2′, the Glu204 residue is in the neutral form and involved in a H-bond (lengths are 1.47 and 1.54 Å for zinc and cobalt in this order) with the oxygen of the original nucleophile. The C−N distance in the substrate is 1.48 and 1.47 Å, for the zinc and cobalt cluster, respectively.
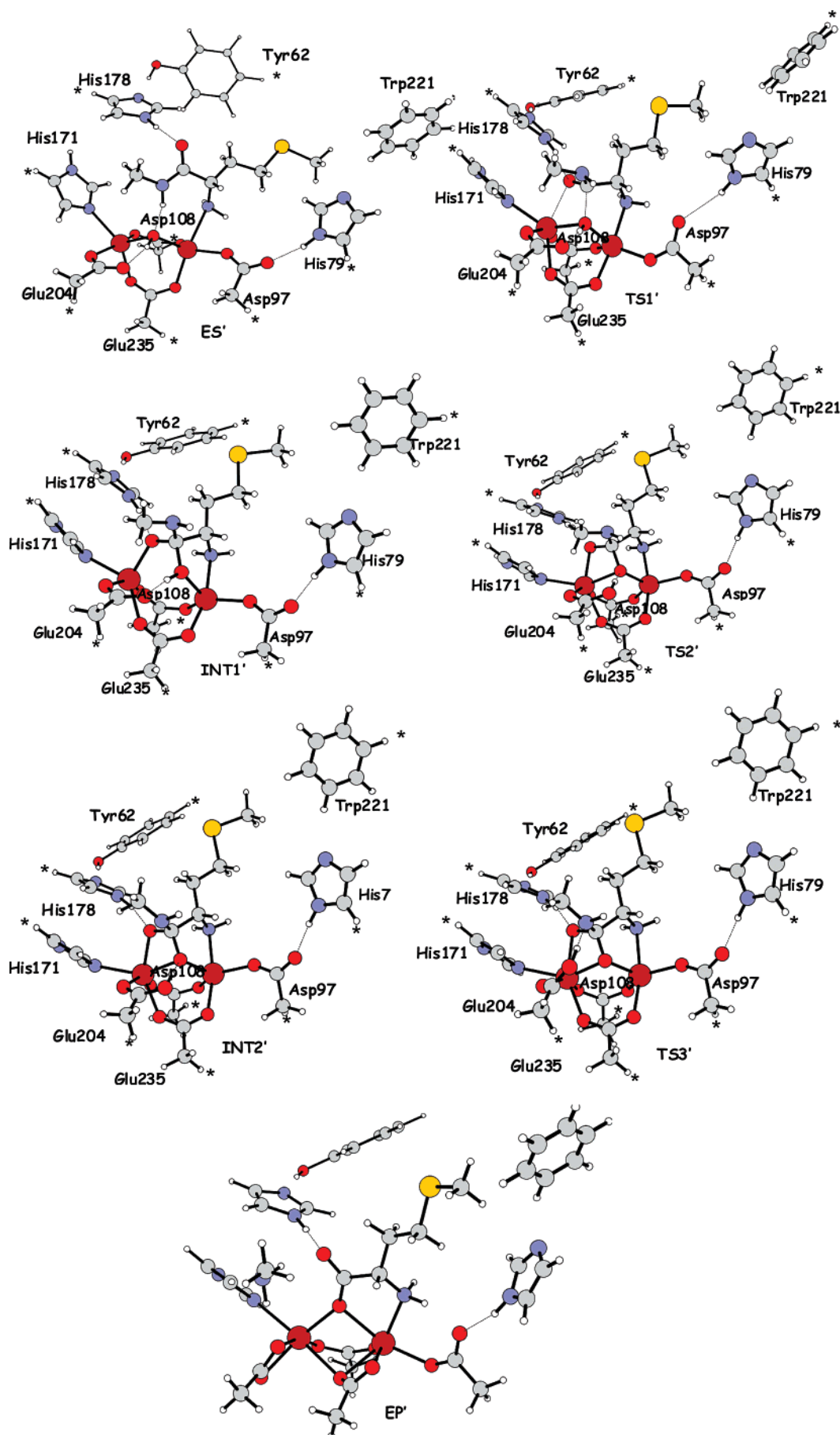
Figure 3. Equilibrium geometries of the stationary points ES′, TS1′, INT1′, TS2′, INT2′, TS3′, and EP′ belonging to mechanism B.

Table 3. Main Geometrical Parameters of Intermediates and Transition States of Mechanism B, for Zinc and Cobalt

	ES′	TS1′	INT1′	TS2′	INT2′	TS3′	EP
Zn1−NH$_{2sub}$	2.46	2.18	2.18	2.18	2.20	2.25	2.18
Zn2−O$_{sub}$	-	2.49	2.06	2.10	2.10	2.17	3.68
Zn2−O$_{Glu204}$	2.07	2.13	2.10	2.26	2.30	2.26	2.19
O$_{OH}$−C$_{sub}$	3.74	1.80	1.48	1.45	1.43	1.38	1.28
C$_{sub}$−O$_{sub}$	1.25	1.29	1.36	1.37	1.37	1.36	1.25
C$_{sub}$−N$_{sub}$	1.33	1.41	1.45	1.47	1.48	1.59	-
Co1−NH$_{2sub}$	2.42	2.15	2.16	2.16	2.17	2.20	2.13
Co2−O$_{sub}$	/	2.81	2.04	2.07	2.05	2.13	3.63
Co2−O$_{Glu204}$	2.04	2.08	2.06	2.17	2.30	2.20	2.19
O$_{OH}$−C$_{sub}$	3.72	1.84	1.49	1.45	1.44	1.38	1.28
C$_{sub}$−O$_{sub}$	1.25	1.27	1.36	1.37	1.37	1.36	1.25
C$_{sub}$−N$_{sub}$	1.34	1.41	1.45	1.47	1.47	1.66	-
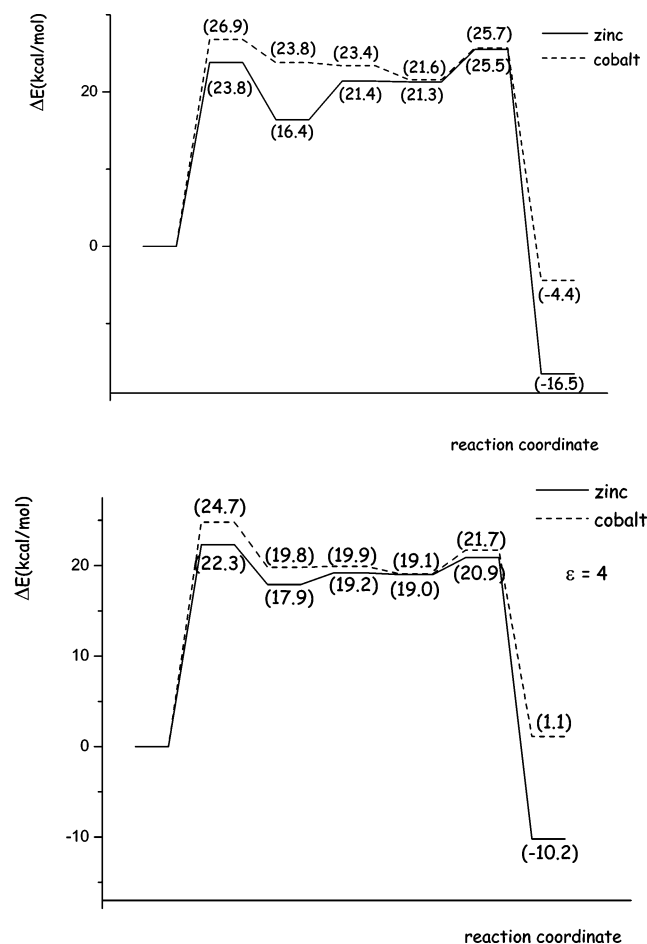
Figure 4. Mechanism B potential energy surfaces for hydrolysis of methionyl-peptide by MetAP, for Zn^{2+} (solid line) and Co^{2+} (dashed line), in the gas phase (on the top) and in the protein environment (on the bottom).

In order to get the final products, the proton transferred to the Glu204 residue must now be shifted toward the amide nitrogen in the substrate. This takes place through the transition state TS3′ (imaginary frequency at 403 and 547 cm^{-1}) in which the simultaneous shift of the proton and the breaking of the C−N bond in the substrate occur. The critical distances of the H−O$_{Glu}$ and H−N$_{sub}$ bonds are 1.15 and 1.41 Å, for zinc, and 1.16 and 1.39 Å, for cobalt, while the C−N bond length in the substrate is 1.59 and 1.66 Å, for zinc and cobalt.

The EP complex is made up by CH$_3$NH$_2$ and methionine products, the latter bound to the enzyme. As can be seen from Figure 3, the B3LYP optimization yields a final complex in which the Glu204 residue binds in a bidentate fashion to the Me2 center and the Glu235 rearranges itself to more strongly interact with the Me1 center, weakening its coordination with the Me2. This is in contrast with the experimental structure of *E. coli* methionine aminopeptidase, in which the complex with the methionine product clearly exhibits a Glu235 residue coordinating both of the metallic centers and the Glu204 involved in a monodentate coordination with the Me2 and hydrogen bound to one of the methionine oxygen atoms, supporting a neutral glutamate.

As far as the energetics is concerned, the rate-determining step in mechanism B can be recognized still in the nucleophilic addition of the bridging OH on the substrate carbonyl carbon (TS1′), but now the barrier height is greater for zinc, 23.8 kcal/mol (solid line), and more or less the same for cobalt (26.9 kcal/mol, dashed line), as compared with the activation energies computed for previous mechanism A (16.8 and 30.5 kcal/mol, for Zn and Co, respectively).

The cluster containing the zinc dication seems to be more reactive than that with Co^{2+}, and the reason can be found again in a more negative charge of the OH nucleophile.

The second transition state describing the shift of the proton from the OH to the Glu204 residue is found at 21.4 (for Zn^{2+}) and 23.4 (for Co^{2+}) kcal/mol above reactants. Contrary to zinc, the energetic profile of cobalt enzyme after the formation of INT1′ is flat and not well resolved. Finally, the scission of the C−N bond leading to the products, taking place through the TS3′ transition state, involves an activation energy of 4.2 (Zn^{2+}) and 4.1 (Co^{2+}) kcal/mol.

Products are found 16.5 and 4.4 kcal/mol below the reference for zinc and cobalt, respectively.

Computations in the protein environment do not introduce meaningful differences with respect to the gas phase. As far as mechanism B is concerned, the nucleophilic addition (TS1′) requires 22.3 and 24.7 kcal/mol and leads to INT1′ lying at 17.9 and 19.8 kcal/mol, in the case of zinc and cobalt, respectively. The protein environment entails a decrease of the barriers of about 2 kcal/mol and destabilizes the Zn-INT1′ species with respect to the gas phase. The relative energies of TS2′ and INT2′ are 19.2 and 19.0 (zinc), and 19.9 and 19.1 (cobalt) kcal/mol. The activation energy to pass from INT2′ to the EP species is computed to be 1.9 kcal/mol, in the case of zinc, and 2.6 kcal/mol, in the case of cobalt. The exothermicity of the hydrolysis reactions seems to be reduced when the surrounding protein is taken into account, since products are found 10.2 kcal/mol below the reference in the case of Zn^{2+} and 1.1 kcal/mol above the reactants, for Co^{2+}.

Conclusions

The catalytic mechanism of the methionine aminopeptidase enzyme was widely investigated at the DF level of theory. The model cluster used to simulate the active site of the enzyme, made up by 108/109 atoms, was large enough to reliably reproduce the hydrolysis of the methionine−peptide substrate.

Four metal cations, Zn, Co, Mn, and Fe, were examined as probable physiological cations in the active site of the enzyme. The two different mechanisms deriving from the presence of a protonated or deprotonated residue Glu204 were taken into account.

The main results can be summarized as follows:

(1) The hydrolytical reaction is made up by the formation of the tetrahedral intermediate, arising from the nucleophilic addition of the metals bridging hydroxide on the substrate carbonyl carbon atom, and by the protonation of the substrate NH, leading to the final C−N bond cleavage in the substrate.

(2) Within mechanism A, involving a protonated Glu204 residue, the computed values of the activation energies necessary to pass from the initial enzyme−substrate complex to the tetrahedral intermediate indicated that the methionine−peptide hydrolysis is kinetically easier in the case of Zn^{2+} rather than for Co^{2+}, Mn^{2+}, and Fe^{2+}. This is essentially due to the greater negative charge density of the OH nucleophile induced by the formation of ionic bonds that the latter establishes with the two zinc cations, other than to the more stressed structure for the zinc enzyme−substrate complex. For the other metals, the covalent contribution to the HO−Me bond is more important than the ionic one.

(3) As far as the deprotonated Glu204 is concerned, results on zinc and cobalt containing clusters again indicated the zinc dication as the one involving the lower activation energies.

(4) The fact that the activation barriers involved in mechanism B in which the Glu204 aminoacid is present in the ionized form are higher than those computed for mechanism A means that the hydrolysis reaction of the methionyl-peptide is kinetically favored when the glutamate residue is in the neutral form.

(5) Based on these findings, methionine aminopeptidase enzyme, whose relevance is related to its involvement in tumor regulation, can be in principle recognized as a dizinc enzyme.

Supporting Information Available: Cartesian coordinates of the stationary points encountered on the Zn−, Co−, Mn−, and Fe−MetAP mechanism A potential energy profiles. Full citation for ref 26. This material is available free of charge via the Internet at http://pubs.acs.org

JA068168T